ChemCatChem

The European Society Journal for Catalysis

Chemistry Europe

European Chemical Societies Publishing

Supported by GECATS GERMAN CATALYSIS SOCIETY

Accepted Article

Title: Understanding the synergistic effects observed when using tethered dual catalysts for heat and light activated catalysis

Authors: Danfeng Wang, Indrek Pernik, Sinead Teresa Keaveney, and Barbara A Messerle

To be cited as: *ChemCatChem* 10.1002/cctc.202000969

Link to VoR: https://doi.org/10.1002/cctc.202000969

WILEY-VCH

RESEARCH ARTICLE WILEY-VCH

Understanding the synergistic effects observed when using tethered dual catalysts for heat and light activated catalysis

Danfeng Wang,[a] Indrek Pernik,[a,b] Sinead T. Keaveney*,[a] and Barbara A. Messerle*,[a,b]

Abstract: Dual catalysis, where two different catalysts work cooperatively to promote a chemical reaction, is an important synthetic approach as it can allow a wide range of unique reactivity to be accessed. Whilst most dual catalysis strategies utilise separate catalysts in the reaction mixture, there is a growing interest in using tethered dual catalysts to increase cooperativity between the catalytic centres. In this current work we sought to determine the origin of the catalytic synergy observed for a series of Ir(I) based complexes tethered to a BODIPY type photocatalyst through different tethering modes. Kinetic analyses revealed that the tethered dual catalysts were more effective at promoting heat activated intermolecular hydroamination than the un-tethered analogues. The tethering mode had a significant influence on the magnitude of this synergistic enhancement observed for the hydroamination reaction, likely due to a combination of steric and electronic ligand effects. Investigations into the effect of the tethered dual catalysts on the light activated oxidation of thioanisole demonstrated that chemical tethering leads to substantial increases in photocatalytic activity, which was once again impacted by the tethering mode. The origin of the observed enhancement was found to be due to both increased singlet oxygen generation through the heavy atom effect, as well as direct involvement of the Ir centre in the oxidation reaction pathway.

Introduction

Catalysis is a powerful tool in synthetic chemistry, with catalytic steps often crucial to the construction of industrially relevant compounds, such as pharmaceuticals, agrochemicals and fine chemicals.[1-3] As a branch of catalysis, photocatalysis is a particularly attractive sustainable approach because light energy is harnessed by the catalyst to fuel chemical transformations. In recent years there has been a surge in interest in developing highly efficient photocatalysts that can promote a wide range of chemical reactions. In particular, combining photocatalysis with other forms of catalysis, often termed 'dual catalysis', has been shown to be an excellent platform for designing novel chemical reactivity.[4-9] Extensive work in this emergent field has allowed numerous multi-catalysis strategies to be developed, where cooperation between the different catalytic centres provides access to new types of chemical reactivity.[4, 10-13]

[a] Dr Danfeng Wang, Dr Indrek Pernik, Dr Sinead T. Keaveney* and Prof. Barbara A. Messerle*
Department of Molecular Sciences
Macquarie University
North Ryde, NSW, 2019, Australia
E-mail: sinead.keaveney@mq,edu,au;
barbara.messerle@sydney.edu.au
[b] *Current address*: Dr Indrek Pernik and Prof. Barbara A. Messerle
School of Chemistry
University of Sydney
Sydney, NSW, 2006, Australia

Supporting information for this article is given via a link at the end of the document.

The majority of the reported dual catalytic systems feature individual catalysts added separately to the reaction mixture, however there is a growing interest in developing single compounds that feature two distinct catalytic sites.[14] Chemically tethering different types of catalysts could allow increased cooperation between the catalytic centres,[15-17] potentially leading to new reactivity being discovered. It is particularly advantageous to utilise this tethering strategy in photocatalysis, as incorporation of 'heavy atoms', such as halides and metals, has been shown to enhance the photocatalytic properties of organic photocatalysts.[18-23] These 'heavy atoms' promote intersystem crossing (ISC) from the singlet to the triplet excited state of the photocatalyst, with this approach widely used to promote reactive singlet oxygen ($^1O_2$) generation through triplet-triplet energy transfer (Figure 1). As such, a variety of tethered photocatalyst – metal complexes have been developed and used in applications that require singlet oxygen generation, such as photocatalysis[24-28] and photodynamic therapy.[26, 29-30]

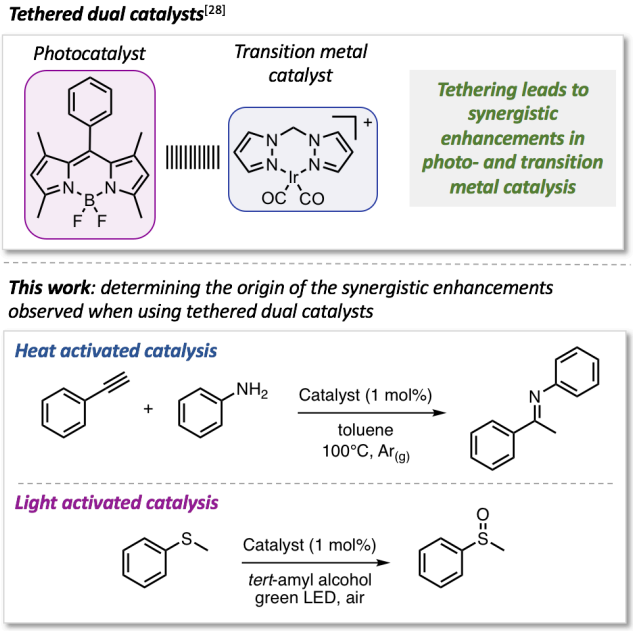

Figure 1: Top: the previously developed tethered dual catalysts, featuring a thermally activated Ir(I) catalyst and a light activated BODIPY-type catalyst. Bottom: the model reactions used in this work to investigate the origin of the synergistic enhancements in catalytic efficiency observed when using tethered dual catalysts.

Despite the increasing use of tethered catalysts that feature both a photocatalyst and a transition metal catalyst,[23, 25, 28, 31-34] there have been limited mechanistic investigations into the origins of the synergistic effects between the catalytic centres. For example, our group recently developed a series of complexes that feature an organic photocatalyst (1,3,5,7-tetramethyl-8-phenyl-4,4-difluoroboradiazaindacene, BDP **1**) tethered to an Ir complex ligated with a bis(pyrazolemethane) (bpm) ligand, Ir(I) **2**

(Figure 1).[28] Three different tethering modes between the parent catalysts BDP **1** and Ir(I) **2** were used, either through a side-side linkage (Ir(I)-BDP SS **3**), a head-head linkage (Ir(I)-BDP HH **4**) or a head-side linkage (Ir(I)-BDP HS **5**). Preliminary catalytic experiments have demonstrated that both catalytic centres remain active in the tethered dual catalysts **3**-**5**,[28] however there is limited understanding of the origin of the cooperative effects on catalysis observed. In this work we present a detailed mechanistic analysis of the tethered dual catalysts **3**-**5** to provide insight into the cooperative effects observed in catalysis, with a particular focus on understanding trends in photocatalytic efficiency.

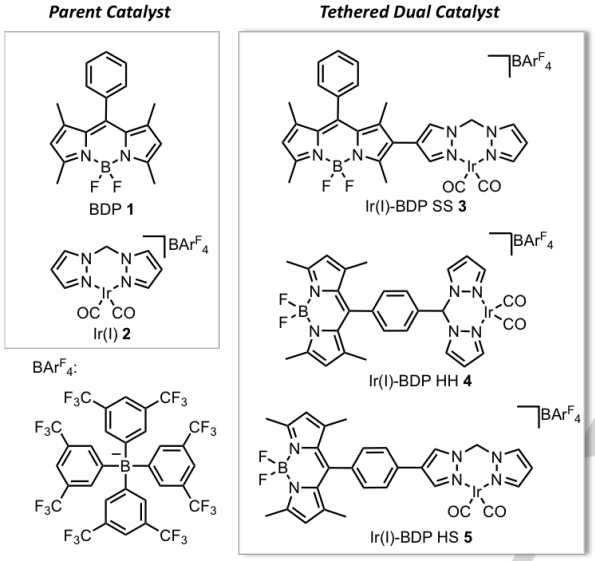

Figure 2: The parent and tethered dual catalysts considered in this work.

Results and Discussion

Initial studies focused on assessing the activity of the Ir(I) species when incorporated in the dual catalysts **3**-**5**. As transition metal catalysed reactions tend to be sensitive to ligand structure and electronics, understanding how the tethering mode effects catalytic efficiency will provide guidance for catalyst development. The activity of the tethered dual catalysts **3**-**5** was investigated using the intermolecular hydroamination reaction between phenylacetylene **6** and aniline **7** as a test reaction. It was found that the catalysts **3**-**5** could effectively promote the formation of the ketimine **8**, suggesting that incorporation of the BDP **1** chromophore into the ligand framework does not deactivate the Ir centre. While the Ir(I)-BDP SS **3** catalyst was found to behave with the same level of activity as the parent catalyst Ir(I) **2**, enhanced activity for the hydroamination reaction was observed for both Ir(I)-BDP HH **4** and Ir(I)-BDP HS **5**, with the head-head linked catalyst **4** being the most efficient (Table 1).

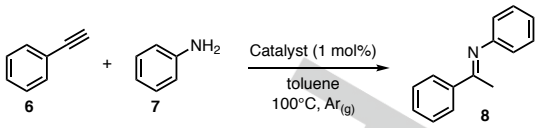

Table 1 Comparisons of the effectiveness of the different catalysts at promoting thermally activated intermolecular hydroamination.

Catalyst	Conversion to product **8** / %		
	1 h	2 h	18 h
BDP **1**	0	0	0
Ir(I) **2**	43 ± 6	55 ± 4	95 ± 1
Ir(I)-BDP SS **3**	38 ± 3	58 ± 6	96 ± 1
Ir(I)-BDP HH **4**	**72 ± 3**	**80 ± 4**	97 ± 1
Ir(I)-BDP HS **5**	57 ± 2	72 ± 5	96 ± 3
BDP **1** + Ir(I) **2**	44 ± 6	57 ± 4	81 ± 8
Ir(I) **9**	43 ± 1	54 ± 4	94 ± 3
No catalyst	0	0	0

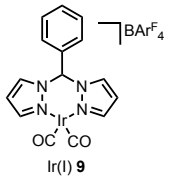

Reaction conditions: Phenylacetylene **6** (24.5 mg, 0.24 mmol), aniline **7** (18.6 mg, 0.2 mmol), catalyst (1 mol%), toluene-d_8 (0.5 mL, dried over sieves) were all combined in a 4 mL vial under an argon atmosphere and heated at 100 °C for the specified time. The average and standard deviation of at least 2 replicate experiments are reported. Conversion to product **8** was determined using ^{1}H NMR spectroscopy relative to the internal standard trimethoxybenzene.

Key control reactions indicated that BDP **1** alone is ineffective at promoting hydroamination (Table 1), and that use of a 1:1 mixture of BDP **1** and Ir(I) **2** gave comparable results to those seen when using just Ir(I) **2**. As such, these data indicate that tethering the BDP **1** and Ir(I) **2** motifs is essential to the rate increase observed, and that direct involvement of BDP **1** in the reaction mechanism is unlikely (rather, it is influencing reactivity through altering the ligand). In addition, use of the Ir(I) **9** catalyst that features a phenyl substituted bpm ligand gave comparable catalytic results to Ir(I) **2**, indicating that the enhancement in catalytic reactivity seen for Ir(I)-BDP HH **4** is not simply due to phenyl substitution on the bpm ligand backbone.

Previous X-ray absorption and infrared spectroscopy measurements of the parent catalyst Ir(I) **2** and the tethered dual catalysts Ir(I)-BDP **3**-**5** suggest that there is an extent of electron transfer from the BDP to the Ir(I) fragment in catalysts Ir(I)-BDP **3**-**5**.[28] In particular, the X-ray absorption spectroscopy data suggests that the greatest extent of electron transfer occurs for Ir(I)-BDP SS **3**, with a 1 eV decrease in edge energy relative to Ir(I) **2**, indicating that the Ir centre in Ir(I)-BDP SS **3** is

significantly more electron rich than Ir(I) **2**. In contrast, Ir(I)-BDP HH **4** and Ir(I)-BDP HS **5** have similar edge energies to Ir(I) **2** (< 0.5 eV decrease relative to Ir(I) **2**), and hence the electron density on Ir is comparable to Ir(I) **2**. Thus, if electron density on the iridium centre was the main factor affecting the hydroamination reaction, we would expect a difference in activity between Ir(I) **2** and Ir(I)-BDP SS **3**. Our experimental data indicate that Ir(I) **2** and Ir(I)-BDP SS **3** are equally effective at promoting the hydroamination reaction between phenylacetylene **6** and aniline **7**, with Ir(I)-BDP HH **4** unexpectedly being the most efficient catalyst (Table **1**). As such, it is unlikely that the electron density on the iridium centre is the main factor affecting the hydroamination reaction between species **6** and **7**.

Overall, while the exact origin of the ligand effect is difficult to confirm, it is clear that the catalyst-catalyst linking mode can influence the catalytic competency of the Ir centre, and that it is an important factor to consider when developing multifunctional catalysts. While the enhancements in catalytic efficiency when using the tethered dual catalysts **3**-**5** for thermally activated intermolecular hydroamination were relatively minor, much more pronounced changes in the efficiency of these catalysts was observed under photocatalytic conditions. The photocatalytic competency of the BDP **1** motif was assessed using the representative oxidation reaction of thioanisole **10** (Table 2).[35-37] Pleasingly, not only was the BDP motif still active in the catalysts **3**-**5**, kinetic analyses showed that their activities were substantially enhanced when compared to the parent BDP **1** catalyst (Table 2 and S3). This effect can be clearly seen by comparing the conversion to the product **11** after 10 hours (Table 2): for BDP **1**, only 8 ± 5% of the product had formed, whereas an approximately 10-fold increase in product formation was seen for Ir(I)-BDP SS **3** (97 ± 1%), with significant enhancements also seen for Ir(I)-BDP HH **4** and Ir(I)-BDP HS **5** (76 ± 5% and 60 ± 8%, respectively).

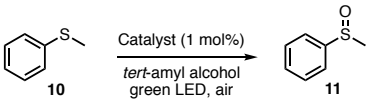

Table 2: Comparisons of the effectiveness of the different catalysts at promoting the photooxidation of thioanisole **10**. [a]Singlet oxygen quantum yields (Φ_Δ) are from reference 28.

Catalyst	Φ_Δ / %[a]	Conversion to product **11** / %		
		6 h	10 h	24 h
BDP **1**	2.6 ± 0.1	5 ± 4	8 ± 5	88 ± 10
Ir(I) **2**		5 ± 1	6 ± 2	4 ± 1
Ir(I)-BDP SS **3**	12.3 ± 0.4	**62 ± 9**	**97 ± 1**	**98 ± 1**
Ir(I)-BDP HH **4**	3.6 ± 0.1	39 ± 5	76 ± 5	98 ± 1
Ir(I)-BDP HS **5**	3.0 ± 0.2	32 ± 7	60 ± 8	98 ± 1
BDP **1** + Ir(I) **2**	3.2 ± 0.1	39 ± 2	81 ± 3	98 ± 1
BDP **1** + Na[$BArF_4$]		5 ± 3	21 ± 12	97 ± 1
bpm-BDP SS **12**		16 ± 1	27 ± 4	99 ± 1
No catalyst		7 ± 1	7 ± 1	4 ± 1

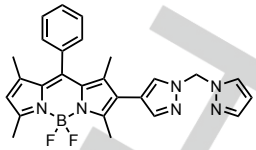

BDP-bpm SS **12**

Reaction conditions: Thioanisole **10** (24.8 mg, 0.2 mmol), catalyst (1 mol%) and, where appropriate, additive (1 mol%) were dissolved in *t*-amyl alcohol (1 mL, saturated with air) in a 4 mL vial under air. The vial was left open (no cap) and irradiated with green LED light for the specified time. The average and standard deviation of at least 2 replicate experiments are reported. Conversion to product **11** was determined by ^{1}H NMR spectroscopy relative to thioanisole **10**. See the supporting information for additional data.

BDP **1** is known to generate $^1O_2$ when irradiated, through energy transfer from the BDP **1** triplet excited state to $^3O_2$.[19, 38-41] As such, the most likely origin of the differing rates of photocatalytic oxidation of the catalysts under consideration is the varying singlet oxygen quantum yield (Φ_Δ) of the photocatalysts, as it would be expected that the rate of thioanisole oxidation would increase when more singlet oxygen is generated. It has been shown previously that the side-side linked catalyst **3** has the highest Φ_Δ (Table 2), due to increased intersystem crossing when using this tethering mode,[28] however, poor correlations between the extent of conversion to the product **11** and either Φ_Δ (Figure S2, R^2 = 0.50) or the rate of $^1O_2$ generation (Figure S3, R^2 = 0.49) were observed. This clearly indicates that the enhanced catalytic efficiency of the dual catalysts **3**-**5**, relative to BDP **1**, is not only due to changes in the extent of $^1O_2$ generation – another factor must also affect activity. This is supported by the key control reaction using a 1:1 mixture of BDP **1** and Ir(I) **2**, which resulted in a significant enhancement in thioanisole **10** oxidation relative to BDP **1**. Since the extent of singlet oxygen generation is the same for BDP **1** and the mixed BDP **1** + Ir(I) **2** system,[28] the rate of singlet oxygen generation is not the only factor contributing to the rate of thioanisole **10** oxidation.

Detailed kinetic studies showed that there was an induction period for BDP **1**, with substantial product formation (> 25%) only occurring after 16 hours, whereas no such effect was seen for catalysts **3**-**5** (Figure S3). While thioanisole oxidation with BDP **1** is known to be sluggish,[37] these low initial conversions could be due to an autocatalytic effect (where the product itself promotes the reaction, with an induction period characteristic of autocatalysis). Spiking the reaction mixtures with the product **11** indicated that the reaction is not autocatalytic for either BDP **1** or Ir(I)-BDP SS **3** (Table S5). Use of a higher reaction concentration resulted in increased thioanisole **10** oxidation (Table S6), suggesting that the induction period observed for BDP **1** could, in part, be due to solvent evaporation, leading to increased reaction rates over time. However, concentration effects do not account for the differences between BDP **1** and the catalysts **3**-**5**. Thus, a possible origin of these different reaction profiles is a change in the reaction mechanism.

As the oxidation of thioanisole can involve either singlet oxygen ($^1O_2$), the superoxide radical anion ($O_2^{\bullet-}$) or both $^1O_2$ and $O_2^{\bullet-}$,[36, 42-45] chemical trapping experiments were performed to

investigate the reaction mechanism. Control reactions in the presence of a singlet oxygen trapping agent[36, 46] resulted in greatly reduced thioanisole **10** oxidation, confirming that $^1O_2$ is involved in the reaction mechanism for both BDP **1** and Ir(I)-BDP SS **3** (Figure 3 and Table S7). However, control reactions using a superoxide radical anion trap[36, 47] also resulted in reaction inhibition, indicating that the photooxidation of thioanisole **10** proceeds through a reaction pathway where both $^1O_2$ and $O_2^{\bullet-}$ are required (Figure 3, Table S7 and S8). Importantly, as $^1O_2$ and $O_2^{\bullet-}$ are involved in thioansiole **10** oxidation for both BDP **1** and Ir(I)-BDP SS **3**, it is unlikely that the differing efficiency of these catalysts is due to changes in the nature of the reactive oxygen species.

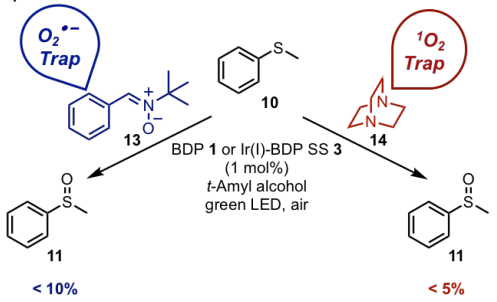

Figure 3: The control reactions used to examine whether a superoxide radical anion (left) or singlet oxygen (right) are involved in the photoxidation of thioanisole **10**. *Reaction conditions*: thioanisole (0.2 mmol), catalyst (0.002 mmol), additive **13** or **14** (0.22 mmol), *t*-amyl alcohol (1 mL, saturated with air) in a 4 mL vial open to air was irradiated with green LED light for 4-24 h, see the Supporting Information for details.

Based on the above data, it is likely that the mechanism of thioanisole oxidation first involves $^1O_2$ generation by the BDP-based photocatalyst, with reactive $^1O_2$ then abstracting an electron from thioanisole **10** to produce the superoxide radical anion and the thioanisole radical cation (Scheme 1). These radicals then react to generate the charge separated persulfoxide ('S^+OO^-') intermediate **15**, which then reacts with another equivalent of thioanisole to deliver the sulfoxide product **11**.[48] This mechanism is supported by previous studies showing that direct electron transfer from a substrate to singlet oxygen can lead to generation of radical ions,[36, 49-50] as well as control reactions we performed with diphenylsulfoxide[51-53] which confirm the formation of persulfoxide intermediate **15** when using catalysts **1** or **3** (see the Supporting Information for more details, Table S9 and S10). In addition, oxidation processes that proceed *via* the charge separated intermediate **15** are known to be promoted by polar solvents due to charge stabilisation,[46, 54-56] and thus the poor reactivity we observed in non-polar toluene (Table S11) further supports the pathway shown in Scheme 1.

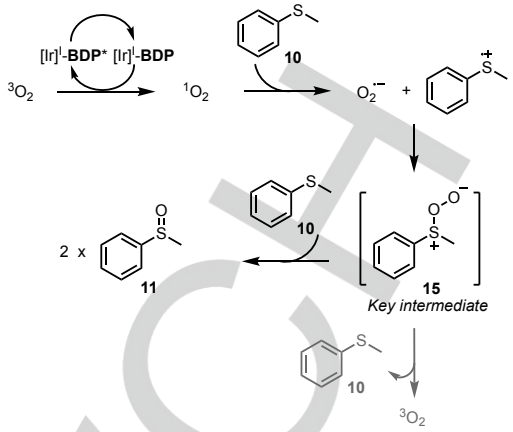

Scheme 1: Proposed mechanism for the photooxidation of thioanisole **10**.

To examine if the BAr^F_4 anion present in catalysts **2**-**5** affects the rate of thioanisole **10** oxidation, a test reaction using a 1:1 mixture of BDP **1** and $NaBAr^F_4$ was performed (Table 2). While a minor enhancement, relative to BDP **1**, was observed, this experiment indicated that the enhancements observed for catalysts **3**-**5** are not simply due to the presence of the BAr^F_4 anion. In addition, use of the bpm-BDP SS ligand as a catalyst suggests that the Ir centre is essential to the observed enhancement (Table 1). A possible explanation is that the Ir centre promotes the reaction between $^1O_2$ and thioanisole either through Ir – O_2 or Ir – S coordination. It has been shown previously that iridium-dioxide species can be generated through reaction of an iridium complex with either singlet[57] or triplet oxygen,[58] and that these types of complexes can oxidise organic compounds.[59] As such, it is possible that dioxide-bound analogues of the iridium based catalysts **2**-**5** form under our reaction conditions. However, as the photooxidation of thioanisole **10** was unsuccessful when using Ir(I) **2** only, it is unlikely that Ir - triplet oxygen coordination is the origin of the rate enhancement seen when using catalysts **3**-**5**, although an Ir - singlet oxygen interaction cannot be excluded.

Conversely, an Ir – S interaction could be promoting thioanisole **10** oxidation, with Ir – S coordination expected to decrease electron density at S. As such, the effect of electronics on the photocatalytic oxidation was examined using substituted thioanisoles. It was found that the oxidation of electron rich 4-methoxythioanisole **17** proceeded more efficiently than electron deficient 4-bromothioanisole **16**, for both BDP **1** and Ir(I)-BDP SS **3**. This indicates that thioanisole oxidation is enhanced when the S moiety is electron rich, and thus an Ir – S interaction could not account for the increased catalytic efficiency observed for catalysts **3**-**5**.

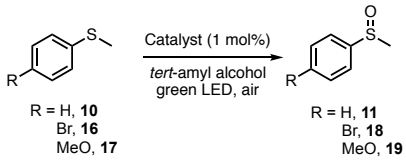

Table 3: The effect of changing the substituent on thioanisole on the rate of photooxidation.

Catalyst	R	Conversion to the oxidised product / %	
		2 h	6 h
BDP **1**	Br	7 ± 1	9 ± 2
	H	5 ± 4	5 ± 4
	OCH_3	15 ± 1	79 ± 2
Ir(I)-BDP SS **3**	Br	16 ± 1	42 ± 2
	H	20 ± 6	62 ± 9
	OCH_3	46 ± 4	99 ± 1

Reaction conditions: Substrate (0.2 mmol), catalyst (1 mol%) were dissolved in *t*-amyl alcohol (1 mL, saturated with air) in a 4 mL vial under air. The vial was left open (no cap) and irradiated with green LED light for the specified time. The average and standard deviation of at least 2 replicate experiments are reported. Conversion to product**s** was determined by ^{1}H NMR spectroscopy relative to starting material. See the supporting information for additional data.

Another possible explanation is that the Ir centre is influencing the reactivity of the charge separated persulfoxide intermediate **15**. It has been well established that this key intermediate can readily decompose *via* undesired intersystem crossing to produce $^3O_2$ and regenerate the starting material (*e.g.* thioanisole **10**).[35, 46, 52, 60-61] However, stabilisation of this intermediate through hydrogen bonding or electrostatic interactions with the 'O$^-$' centre can reduce the extent of decomposition, and lead to increased formation of the desired sulfoxide product.[35, 51-52, 60, 62-66] Hence, it is possible that the observed increase in thioanisole **10** oxidation arises from stabilisation of the persulfoxide intermediate **15** by the cationic iridium centre, as shown in Scheme 2.

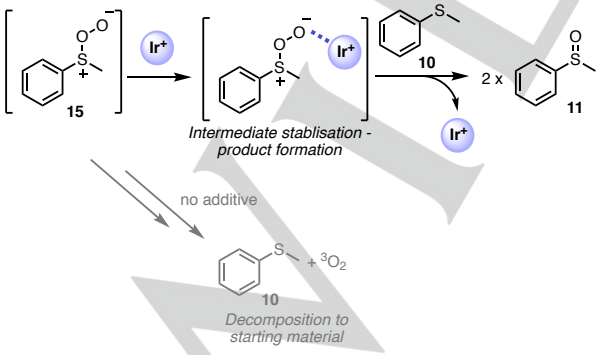

Scheme 2: Schematic illustration of the proposed interaction between the cationic iridium centre and the persulfoxide intermediate **15**.

To examine whether an Ir - 'O$^-$' interaction is increasing the rate of thioanisole **10** oxidation, a series of reactions were performed using BDP **1** and Ir-based additives, with increased reactivity observed in all cases, relative to BDP **1** only (Table 4). The most pronounced enhancement was seen when using the $Ir^{(III)}Cl_3.xH_2O$ additive, suggesting that the more electron deficient the iridium centre is, the greater the extent of Ir - 'O$^-$' interaction and thus the greater the Ir – intermediate **15** stabilisation. This 'cation' - 'O$^-$' interaction was further confirmed using a $NaBAr^F{}_4$ additive, where it would be expected that the cationic Na^+ is also able to stabilise the persulfoxide intermediate **15**.[51] While the effect was less pronounced than when using Ir-based additives, a significant enhancement in thioanisole **10** oxidation was also observed when using large amounts of a $NaBAr^F{}_4$ additive (Table 4).

Table 4: The effect of additives on the rate of thioanisole **10** photooxidation.

Catalyst	Additive	Conversion to product **11** / %		
		6 h	10 h	24 h
BDP **1**	-	5 ± 4	8 ± 5	88 ± 10
BDP **1**	Ir(I) **2** (1 mol%)	39 ± 2	81 ± 3	98 ± 1
BDP **1**	$[Ir^{(I)}(COD)Cl]_2$ (1 mol%)	12 ± 1	17 ± 5	95 ± 5
BDP **1**	$Ir^{(III)}Cl_3.xH_2O$ (1 mol%)	84 ± 16	100 ± 0	100 ± 0
BDP **1**	$NaBArF_4$ (1 mol%)	5 ± 3	21 ± 12	97 ± 1
BDP **1**	$NaBArF_4$ (10 mol%)*	12 ± 3	53 ± 10	97 ± 0
BDP **1**	$NaBArF_4$ (100 mol%)*	39 ± 9	93 ± 1	93 ± 1

Reaction conditions: Thioanisole **10** (24.8 mg, 0.2 mmol), BDP **1** (1 mol%) and where appropriate, an additive was dissolved in *t*-amyl alcohol (1 mL, saturated with air) in a 4 mL vial under air. The vial was left open (no cap) and irradiated with green LED light for the specified time. The average and standard deviation of at least 2 replicate experiments are reported. Conversion to product **11** was determined by ^{1}H NMR spectroscopy relative to thioanisole **10** (*as well as the small amount of over-oxidised sulfone product ($PhSO_2CH_3$) observed when using 10 and 100 mol% of $NaBAr^F{}_4$). See the supporting information for additional data.

It should be highlighted that if the *only* factor affecting thioanisole **10** oxidation was intermediate **15** stabilisation, the more electron deficient Ir(I) **2** would be expected to be more active than Ir(I)-BDP SS **3**. However, the opposite trend in reactivity is observed (Table 2), which is likely due to Ir(I)-BDP SS **3** being more effective at generating singlet oxygen than Ir(I) **2**. As such, these results suggest that the ability of the catalyst to promote thioanisole **10** is determined by a complex interplay of two different factors – the ability to stabilise intermediate **15** and the rate at which singlet oxygen is generated.

Overall, it can be concluded that the increased rate of thioanisole **10** oxidation observed when using the tethered dual catalysts **3**-**5**, relative to BDP **1**, is due to a combination the iridium centre: 1) increasing singlet oxygen generation through the heavy atom effect; and 2) stabilising the persulfoxide intermediate **15**, which reduces the extent of unproductive

decomposition to thioanisole **10**. This is important as it demonstrates that tethering a metal complex to an organic photocatalyst can result in synergistic effects beyond simply the heavy atom effect.

Conclusions

In summary, we have performed detailed mechanistic analyses of a series of tethered Ir(I)-BDP catalysts to understand the effects of tethering on both thermal and photo activated catalytic processes. Kinetic studies on the thermally activated intermolecular hydroamination reaction between phenylacetylene **6** and aniline **7** revealed that chemical tethering leads to enhanced catalytic activity for catalysts **3**-**5**, relative to Ir(I) **2**. The mode of tethering was found to affect catalytic efficiency, with the 'head-head' tethered catalyst Ir(I)-BDP HH **4** being most effective. It was demonstrated that the BDP **1** motif is not directly involved in the reaction mechanism, and comparison of the catalytic data with reported X-ray absorption spectroscopy and infrared data for catalysts **2**-**5** indicate that the changes in catalytic efficiency aren't simply due to an electronic effect. As such, the enhancements in the intermolecular hydroamination reaction between compounds **6** and **7** seen when using catalysts **3**-**5**, relative to Ir(I) **2**, are likely due to a ligand effect, where both the steric and electronic properties of the ligand contribute.

Detailed kinetic investigations on the photo-activated oxidation of thioanisole **10** indicate that a significant increase in photocatalytic efficiency was observed for catalysts **3**-**5**, relative to BDP **1**. In this case the side-side linked catalyst Ir(I)-BDP SS **3** was most effective, in contrast to Ir(I)-BDP HH **4** which was most effective for thermally activated catalysis, highlighting that the optimum catalyst tethering mode can be dependent on reaction type. As it is well known that tethering 'heavy atoms', such as Ir(I) **2**, to BDP **1** can increase the extent of reactive singlet oxygen generation, differing abilities of the catalysts to generate $^1O_2$ was the most likely origin of the changes in photocatalytic efficiency observed. Surprisingly, there was a poor correlation (R^2 = 0.5) between the extent of thioanisole **10** oxidation and the singlet oxygen generating ability of the catalysts, suggesting that the origin of the rate enhancement when using catalysts **3**-**5** is complex.

A range of mechanistic investigations was used to further probe the origin of the synergistic catalytic effects seen for thioansiole **10** oxidation. Our studies suggest that the Ir(I) moiety is directly involved in the reaction mechanism, and promotes thioanisole **10** oxidation through stabilisation of the charge separated persulfoxide ('S^+OO^-') intermediate **15**. As such, the Ir(I) motif has the dual role of enhancing singlet oxygen generation and stabilising the key intermediate **15**, resulting in the significant enhancement in photocatalytic activity observed for the tethered dual catalysts **3**-**5**. This is important as it highlights that it is necessary to assess whether there is direct involvement of the metal centre in the reaction mechanism when using functionalised photocatalysts and tethered dual catalysts. In addition, this works sheds light on previous photocatalytic reactions where little correlation between the rates of singlet oxygen generation and catalytic efficiency were observed,[21, 28] suggesting that the metal complexes used to increase singlet oxygen generation can be non-innocent.

Experimental Section

See the Supporting Information for all experimental details, additional catalytic data and control experiments.

Acknowledgements

The authors would like to thank the Chemical Analysis Facility at Macquarie University, in particular Dr Nicole Cordina and Dr Remi Rouquette. DW acknowledges the support of Macquarie University through the iMQRES scholarship program. STK acknowledges the support of Macquarie University through the receipt of a Macquarie University Research Fellowship (MQRF).

Keywords: BODIPY • dual catalysis • mechanism • photooxidation

References

[1] C. A. Busacca, D. R. Fandrick, J. J. Song, C. H. Senanayake, *Adv. Synth. Catal.* **2011**, *353*, 1825-1864.
[2] P. Devendar, R.-Y. Qu, W.-M. Kang, B. He, G.-F. Yang, *J. Agr. Food. Chem.* **2018**, *66*, 8914-8934.
[3] D. Pflaesterer, A. S. K. Hashmi, *Chem. Soc. Rev.* **2016**, *45*, 1331-1367.
[4] K. L. Skubi, T. R. Blum, T. P. Yoon, *Chem. Rev.* **2016**, *116*, 10035-10074.
[5] M. N. Hopkinson, B. Sahoo, J. L. Li, F. Glorius, *Chem.: Eur. J.* **2014**, *20*, 3874-3886.
[6] J. Du, K. L. Skubi, D. M. Schultz, T. P. Yoon, *Science* **2014**, *344*, 392-396.
[7] J. C. Tellis, C. B. Kelly, D. N. Primer, M. Jouffroy, N. R. Patel, G. A. Molander, *Acc. Chem. Res.* **2016**, *49*, 1429-1439.
[8] M. Rueping, R. M. Koenigs, K. Poscharny, D. C. Fabry, D. Leonori, C. Vila, *Chem.: Eur. J.* **2012**, *18*, 5170-5174.
[9] J. C. Tellis, D. N. Primer, G. A. Molander, *Science* **2014**, *345*, 433-436.
[10] D. Wang, N. Zhu, P. Chen, Z. Lin, G. Liu, *J. Am. Chem. Soc.* **2017**, *139*, 15632-15635.
[11] C. K. Prier, D. A. Rankic, D. W. MacMillan, *Chem. Rev.* **2013**, *113*, 5322-5363.
[12] J. Twilton, C. Le, P. Zhang, M. H. Shaw, R. W. Evans, D. W. C. MacMillan, *Nat. Rev. Chem.* **2017**, *1*, 0052.
[13] A. E. Allen, D. W. C. MacMillan, *Chem. Sci.* **2012**, *3*, 633-658.
[14] X. Lang, J. Zhao, X. Chen, *Chem. Soc. Rev.* **2016**, *45*, 3026-3038.
[15] D. Ghosh, H. Takeda, D. C. Fabry, Y. Tamaki, O. Ishitani, *ACS Sustain. Chem. Eng.* **2019**, *7*, 2648-2657.
[16] K. Mori, M. Kawashima, H. Yamashita, *Chem. Commun.* **2014**, *50*, 14501-14503.
[17] A. Inagaki, S. Edure, S. Yatsuda, M. Akita, *Chem. Commun.* **2005**, 5468-5470.

[18] X.-F. Zhang, X. Yang, *J. Phys. Chem. B* **2013**, *117*, 5533-5539.
[19] A. Loudet, K. Burgess, *Chem. Rev.* **2007**, *107*, 4891-4932.
[20] V. Lakshmi, M. Ravikanth, *Dalton Trans.* **2012**, *41*, 5903-5911.
[21] W. Li, L. Li, H. Xiao, R. Qi, Y. Huang, Z. Xie, X. Jing, H. Zhang, *Rsc Adv.* **2013**, *3*, 13417-13421.
[22] J. Zhao, K. Xu, W. Yang, Z. Wang, F. Zhong, *Chem. Soc. Rev.* **2015**, *44*, 8904-8939.
[23] D. Wang, N. S. D. Solomon, I. Pernik, B. A. Messerle, and S. T. Keaveney, *Aust. J. Chem* **2020**, DOI: 10.1071/CH19569.
[24] S. Guo, L. Ma, J. Zhao, B. Küçüköz, A. Karatay, M. Hayvali, H. G. Yaglioglu, A. Elmali, *Chem. Sci.* **2014**, *5*, 489-500.
[25] D. Chao, M. Zhao, *ChemSusChem* **2017**, *10*, 3358-3362.
[26] W. Iali, P. H. Lanoe, S. Torelli, D. Jouvenot, F. Loiseau, C. Lebrun, O. Hamelin, S. Ménage, *Angew. Chem., Int. Ed.* **2015**, *54*, 8415-8419.
[27] W. Wu, J. Sun, X. Cui, J. Zhao, *J. Mater. Chem. C* **2013**, *1*, 4577-4589.
[28] D. Wang, R. Malmberg, I. Pernik, K. Venkatesan, S. K. K. Prasad, T. W. Schmidt, S. T. Keaveney, B. A. Messerle, *Chem. Sci.* **2020**, *11*, 6256-6267.
[29] N. E. Aksakal, E. Tanrıverdi Eçik, H. H. Kazan, G. Yenilmez Çiftçi, F. Yuksel, *Photochem. Photobiol. Sci.* **2019,** *18*, 2012-2022.
[30] T. Wang, Y. Hou, Y. Chen, K. Li, X. Cheng, Q. Zhou, X. Wang, *Dalton Trans.* **2015**, *44*, 12726-12734.
[31] Y. Yamazaki, K. Ohkubo, D. Saito, T. Yatsu, Y. Tamaki, S. i. Tanaka, K. Koike, K. Onda, O. Ishitani, *Inorg. Chem.* **2019**, *58*, 11480-11492.
[32] Y.-H. Luo, L.-Z. Dong, J. Liu, S.-L. Li, Y.-Q. Lan, *Coord. Chem. Rev.* **2019**, *390*, 86-126.
[33] A. Nakada, K. Koike, T. Nakashima, T. Morimoto, O. Ishitani, *Inorg. Chem.* **2015**, *54*, 1800-1807.
[34] A. Nakada, K. Koike, K. Maeda, O. Ishitani, *Green Chem.* **2016**, *18*, 139-143.
[35] J. J. Liang, C. L. Gu, M. L. Kacher, C. S. Foote, *J. Am. Chem. Soc.* **1983**, *105*, 4717-4721.
[36] C. Ye, Y. Zhang, A. Ding, Y. Hu, H. Guo, *Sci. Rep.* **2018**, *8*, 2205.
[37] W. Li, Z. Xie, X. Jing, *Catal. Commun.* **2011**, *16*, 94-97.
[38] G. Ulrich, R. Ziessel, A. Harriman, *Angew. Chem., Int. Ed.* **2008**, *47*, 1184-1201.
[39] T. Yogo, Y. Urano, Y. Ishitsuka, F. Maniwa, T. Nagano, *J. Am. Chem. Soc.* **2005**, *127*, 12162-12163.
[40] M. A. Filatov, S. Karuthedath, P. M. Polestshuk, S. Callaghan, K. J. Flanagan, T. Wiesner, F. Laquai, M. O. Senge, *ChemPhotoChem* **2018**, *2*, 606-615.
[41] G. Duret, R. Quinlan, P. Bisseret, N. Blanchard, *Chem. Sci.* **2015**, *6*, 5366-5382.
[42] J. Dad'ová, E. Svobodová, M. Sikorski, B. König, R. Cibulka, *ChemCatChem* **2012**, *4*, 620-623.
[43] T. Neveselý, E. Svobodova, J. Chudoba, M. Sikorski, R. Cibulka, *Adv. Synth. Catal.* **2016**, *358*, 1654-1663.
[44] J. Li, Y. Chen, X. Yang, S. Gao, R. Cao, *J. Catal.* **2020**, *381*, 579-589.
[45] Y. Gao, H. Xu, S. Zhang, Y. Zhang, C. Tang, W. Fan, *Org. Biomol. Chem.* **2019**, *17*, 7144-7149.
[46] E. Baciocchi, T. D. Giacco, F. Elisei, M. F. Gerini, M. Guerra, A. Lapi, P. Liberali, *J. Am. Chem. Soc.* **2003**, *125*, 16444-16454.
[47] S.-U. Kim, Y. Liu, K. M. Nash, J. L. Zweier, A. Rockenbauer, F. A. Villamena, *J. Am. Chem. Soc.* **2010**, *132*, 17157-17173.
[48] E. Baciocchi, C. Crescenzi, O. Lanzalunga, *Tetrahedron* **1997**, *53*, 4469-4478.
[49] M. Hayyan, M. A. Hashim, I. M. Al Nashef, *Chem. Rev.* **2016**, *116*, 3029-3085.
[50] I. Saito, T. Matsuura, K. Inoue, *J. Am. Chem. Soc.* **1981**, *103*, 188-190.
[51] E. L. Clennan, W. Zhou, J. Chan, *J. Org. Chem* **2002**, *67*, 9368-9378.
[52] E. Baciocchi, C. Chiappe, T. Del Giacco, C. Fasciani, O. Lanzalunga, A. Lapi, B. Melai, *Org. Lett.* **2009**, *11*, 1413-1416.
[53] Z. Cheng, P. Sun, A. Tang, W. Jin, C. Liu, *Org. Lett.* **2019**, *21*, 8925-8929.
[54] M. Kirihara, J. Yamamoto, T. Noguchi, Y. Hirai, *Tetrahedron Lett.* **2009**, *50*, 1180-1183.
[55] J. Jiang, R. Luo, X. Zhou, Y. Chen, H. Ji, *Adv. Synth. Catal.* **2018**, *360*, 4402-4411.
[56] S. M. Bonesi, I. Manet, M. Freccero, M. Fagnoni, A. Albini, *Chem.: Eur. J.* **2006**, *12*, 4844-4857.
[57] M. Selke, C. S. Foote, *J. Am. Chem. Soc.* **1993**, *115*, 1166-1167.
[58] C. Schiwek, J. Meiners, M. Förster, C. Würtele, M. Diefenbach, M. C. Holthausen, S. Schneider, *Angew. Chem., Int. Ed.* **2015**, *54*, 15271-15275.
[59] M. P. del Río, P. Abril, J. A. López, M. Sodupe, A. Lledós, M. A. Ciriano, C. Tejel, *Angew. Chem., Int. Ed.* **2019**, *58*, 3037-3041.
[60] E. L. Clennan, *Acc. Chem. Res.* **2001**, *34*, 875-884.
[61] N. Sawwan, A. Greer, *Chem. Rev.* **2007**, *107*, 3247-3285.
[62] S. M. Bonesi, M. Fagnoni, A. Albini, *J. Org. Chem* **2004**, *69*, 928-935.
[63] S. M. Bonesi, A. Albini, *J. Org. Chem.* **2000**, *65*, 4532-4536.
[64] S. M. Bonesi, M. Mella, N. d'Alessandro, G. G. Aloisi, M. Vanossi, A. Albini, *J. Org. Chem.* **1998**, *63*, 9946-9955.
[65] X. Lang, W. R. Leow, J. Zhao, X. Chen, *Chem. Sci.* **2015**, *6*, 1075-1082.
[66] X. Lang, W. Hao, W. R. Leow, S. Li, J. Zhao, X. Chen, *Chem. Sci.* **2015**, *6*, 5000-5005.

10.1002/cctc.202000969

WILEY-VCH

Entry for the Table of Contents (Please choose one layout)

RESEARCH ARTICLE

Insight into tethered dual catalyst function. This work presents a series of mechanistic investigations into the origin of the synergistic enhancements observed when using tethered dual catalysts to promote both light and heat activated catalytic processes. The iridium complex was shown to enhance photocatalysis through both increased singlet oxygen generation *via* the heavy atom effect, as well as preventing decomposition of a key intermediate through Ir - O interaction.

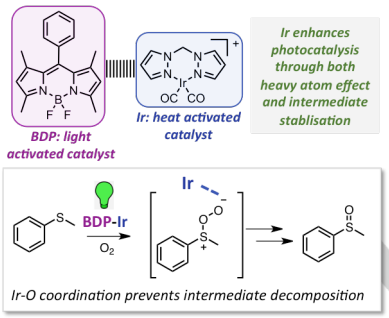

Danfeng Wang, Indrek Pernik, Sinead T. Keaveney and Barbara A. Messerle**

Page No. – Page No.

Understanding the synergistic effects observed when using tethered dual catalysts for heat and light activated catalysis